Expected energy fluxes onto ITER Plasma Facing Components during disruption thermal quenches from multi-machine data comparisons

A. Loarte 1), P. Andrew 2), G.F. Matthews 2), J. Paley 2), V. Riccardo 2), T. Eich 3), C. Fuchs 3), O. Gruber 3), A. Herrmann 3), G.Pautasso 3), G. Counsell 2), G. Federici 4), K.H. Finken 5), G. Maddaluno 6), D. Whyte 7,8), ASDEX Upgrade Team, EFDA-JET Collaborators, FTU Team, MAST Team, TEXTOR-DED Team and DIII-D Team

[1]*EFDA Close Support Unit Garching, Boltmannstr.2, D-85748 Garching bei München, Germany*
[2]*Euratom-UKAEA Fusion Association, Culham Science Centre, Abingdon OX113 3EA, United Kingdom*
[3]*Association Euratom-Max-Planck Institut für Plasmaphysik, Boltmannstr.2, D-85748 Garching bei München, Germany*
[4]*ITER International Team, Garching Working Site, Boltmannstr.2, D-85748 Garching bei München, Germany*
[5]*Association Euratom- Institut für Plasmaphysik Jülich, D-5245 Jülich, Germany*
[6]*Association Euratom-ENEA Frascati, via Enrico Fermi 45, 00044 Frascati, Italy*
[7]*Dept. Engineering Physics, University of Wisconsin-Madison, 1500 Engineering Dr., Madison, WI 53706, USA*
[8]*DIII-D National Fusion Facility, P.O. Box 85608, San Diego, CA 92186, USA*

Abstract. A comparison of the power flux characteristics during the thermal quench of plasma disruptions among various tokamak experiments has been carried out and conclusions for ITER have been drawn. It is generally observed that the energy of the plasma at the thermal quench is much smaller than that of a full performance plasma. The timescales for power fluxes onto PFCs during the thermal quench, as determined by IR measurements, are found to scale with device size but not to correlate with pre-disruptive plasma characteristics. The profiles of the thermal quench power fluxes are very broad for diverted discharges, typically a factor of 5 – 10 broader than that measured during "normal" plasma operation, while for limiter discharges this broadening is absent. The combination of all the above factors is used to derive the expected range of power fluxes on the ITER divertor target during the thermal quench. The new extrapolation derived in this paper indicates that the average disruption in ITER will deposit an energy flux approximately one order of magnitude lower than previously thought. The evaluation of the ITER divertor lifetime with these revised specifications is carried out.

1. Introduction.

The expected energy fluxes to plasma facing components (PFCs) during disruptions in ITER are in the range of tens of GW/m^2 for timescales ~ 1 ms and can, therefore, lead to substantial damage of these components. This, in turn, is a major driver for the choice of PFC materials in ITER, as the possible disruption–associated damage can lead to a substantial lifetime reduction, in particular for metallic PFCs [1]. Energy fluxes of this magnitude cause severe material damage (e.g., evaporation for CFC or melting of W) to the divertor targets. Although some mitigating effects may arise due to the formation of a vapour shield, its behaviour is still uncertain [2]. Therefore, under disruptions, severe metal melting and splashing may occur, thus limiting the lifetime and power handling performance of subsequent plasma operation for a W divertor target for ITER [1].

Previous studies for ITER concluded that the most critical phase of the disruption process, in this respect, is the thermal quench of plasma disruptions [3]. Based on the scarce experimental data available at the time, the following specifications were derived for the disruption energy fluxes during the ITER thermal quench [4] :

a) Plasma thermal energy at the thermal quench $W_{th}^{t.q.}$ ~ 350 MJ, i.e., the energy of the full performance ITER Q_{DT} = 10 reference scenario.

b) Timescale of the thermal quench energy flux ~ 0.4 – 2.2 ms, with ~ 1 ms a typical value.

c) Energy deposition area ~ 3 $A_{s.s.}$, where $A_{s.s.}$ is the divertor effective area for energy deposition for plasma operation in the reference scenario conditions. For ITER, $A_{s.s.}$

is approximately 3.5 m^2 [5]. In agreement with this specification, only up to 0.2 $W_{th}^{t.q.}$ was expected to flow outside the divertor target region (divertor baffles and first wall).

Since these initial studies, there has been substantial progress in the experimental understanding of the energy fluxes that take place during disruptions in tokamak devices. This has been associated with a significant improvement of the diagnostics required for their determination, as well as with the increase of the experimental time dedicated to study disruption physics in most tokamak devices. This paper summarises the above progress, concentrating on the comparison of results among various devices, with a view to provide an estimate for the energy fluxes during the thermal quench of disruptions in ITER. The experiments/analysis reported in this paper form part of the co-ordinated research activities of the European Union Task Force on Plasma-Wall Interactions and of the International Tokamak Physics Activity MHD, Disruption & Control and Divertor and SOL Physics Topical Groups.

2. Plasma evolution and PFC energy fluxes in the approach to disruptions.

The dynamics of the plasma before the disruption depends on the cause of the instability that takes the plasma from its steady-state condition into an unstable situation. This finally ends up in an MHD unstable current profile causing the disruption itself. Typical instability triggers are : thermal instabilities by excessive density or impurity content, growth of MHD modes (such as NTMs), etc. As a consequence of these instabilities, the plasma suffers a deterioration of its energy confinement well in advance of the gross MHD instability that causes the current profile flattening and the thermal quench itself. This phenomenology has two major implications with respect to the flux of energy onto PFCs during the pre-disruptive phases and during the thermal quench itself : a) Prior to the disruption, the power flux to PFCs is enhanced with respect to that for steady state conditions and b) the plasma energy at the time of the thermal quench is substantially smaller than that of the full performance plasma. The only known exceptions to this general picture are pure vertical displacement events (VDEs) and disruptions of JET and DIII-D discharges with internal transport barriers (ITBs), in which the radial pressure gradient ($\vec{\nabla}_r p$) exceeds MHD limits. In these cases the plasma reaches the thermal quench, while maintaining very high thermal energy.

Details of the plasma parameter evolution for three disruptions in JET [6, 7] and MAST [8] are shown in Fig. 1.a-c, which are representative of the observations in most devices. Fig. 1.a corresponds to a JET discharge in which the plasma undergoes a L-H transition during the additional heating ramp-down leading to a density limit disruption. In this case the pre-disruption phase lasts for a substantial length of time (~ 1s), in which the plasma energy decreases from 6 to 2 MJ. During this long pre-disruption phase, large divertor power fluxes are measured (in particular at the L-H transition) that are comparable (albeit lower) than those at the thermal quench. This figure also shows that the divertor power fluxes during the thermal quench are comparable to that during Type I ELMs in the steady phase of the discharge. This observation, which will be discussed in more detail later, highlights the fact that the power fluxes to PFCs during the disruption thermal quench in most divertor tokamaks are not significantly different from those occurring in other transient events, such as ELMs. The timing and duration of the large pre-disruptive power fluxes is correlated with the type of disruption and device size, as can be seen by comparing the measurements in Fig.1.a with those in Fig.1.b for a mode-lock triggered disruption in MAST. In general, the time evolution of the pre-disruptive plasma energy losses is slower in larger devices and the magnitude of the associated fluxes smaller compared to those at the thermal quench itself. There are indeed few disruption types in which no significant pre-disruption fluxes to PFCs are measured at all, such as in pure VDEs and high $\vec{\nabla}_r p$ ITBs in JET [9] and DIII-D [10], as shown in Fig. 1.c. In this case, the only noticeable transient energy flux to the divertor is measured during the thermal quench. It is important to note that, although the peak divertor power flux at the divertor measured in other pre-disruptive events and/or transients (such as ELMs) may be comparable to that at the thermal quench, the total

amount of energy that reaches the divertor (and other PFCs) at the thermal quench is much larger than that in the transients. This is due to the spatial distribution of the energy on PFCs during the thermal quench, which has a very broad footprint, as it will be discussed in detail in Sec. 3.

With a view to the extrapolation of the disruption energy fluxes to ITER and the associated PFC material damage we can conclude that, on the basis of present experimental evidence, the dominant power fluxes are those that occur during the thermal quench for most disruptions. However, in some cases, other pre-disruptive events can cause similar power fluxes onto the divertor target. In these cases, the temperature increase at the divertor target caused by these pre-disruptive events will be similar to that of the thermal quench and the expected material damage comparable. No systematic study has been carried out to determine how often and for which disruption types this occurs. On the basis of existing (but scarce) JET and MAST data, large pre-disruptive transient fluxes are only observed in discharges in which the plasma suffers a fast deterioration of performance before the thermal quench either : a) by the presence of a large MHD mode or b) by a sudden decrease of the additional heating while the plasma is in a high confinement Type I ELMy H-mode regime, such as that shown in Fig. 1.a. In this case the plasma returns to L-mode directly from Type I ELMy H-mode (skipping a long Type III ELMy H-mode phase, which is present in slower transitions). The divertor power fluxes associated with this transition are comparable with those of the thermal quench itself, but this type of transition will not take place in high-energy ITER plasmas. The sudden decrease of the input power required to trigger a fast Type I ELMy H-mode → L-mode is unlikely to occur in the Q_{DT} = 10 ITER reference regime, as the input power to the plasma is dominated by the alpha particle heating and will, therefore, change only in timescales comparable to the energy/particle confinement times.

Due to the pre-disruptive energy confinement deterioration described above, the plasma energy at the time of the thermal quench is substantially lower than that of the full performance plasma. Histograms for the ratio of the plasma energy at the thermal quench to that at full plasma performance for a large ensemble of disruptive discharges in JET [9] and ASDEX Upgrade [11] are shown in Figs. 2.a-b. Similar values are found in MAST [8] and DIII-D [12] for density limit ($W_{t.q.}/W_{dia}^{max}$ ~ 0. 55 (MAST), 0.16 ~ (DIII-D)) and locked-mode disruptions ($W_{t.q.}/W_{dia}^{max}$ ~ 0. 35 (MAST)). From this analysis, the energy of the plasma at the time of the thermal quench in JET is typically around ~ 25 ± 12% of that of a full performing plasma, where 12 % is the standard deviation of the distribution (~ 40 ± 22% in ASDEX Upgrade). The usual exceptions to this rule are pure VDEs and high $\bar{\nabla}_r p$ ITB collapses in JET and DIII-D [9, 10, 12]. Normalising to the maximum energy of the plasma in the discharge introduces device specific features in the study. This is due to the different disruption amelioration measures, or fail-safe operation actions, taken by the plant in anticipation of the impending disruption, which are different across the various devices. In a attempt to eliminate this machine dependent effect, we have taken as reference plasma energy for normalisation of the JET observations the extrapolated plasma energy following the ITER-98(y,2) scaling. That is, the energy that the plasma would have if it maintained good H-mode confinement (H_{98} = 1) up to the thermal quench. In ITER, this would correspond to a situation in which no remedial pre-disruptive action is taken by the plant systems. With this second normalisation, the plasma energy at the thermal quench in JET is ~ (42 ± 20%) of that of a high confinement H-mode (with the same plasma parameters as those of the discharge at the thermal quench). Although this second analysis provides a more device independent estimate for ITER, it seems unreasonable to think that no pre-disruptive remedial action will be taken in ITER. In this sense, the distributions shown in Figs. 2.a-b provide a more realistic estimate of what to expect in ITER. It is important to note that normalising to the ITER-98(y,2) scaling leads to normalised values of the energy at the thermal quench being larger than 1 for high $\bar{\nabla}_r p$ ITB disruptions. This is caused by the fact that the ITER-98(y,2) is a H-mode energy confinement scaling law and does not describe ITB energy confinement adequately. This inadequacy is exacerbated for times

close to the thermal quench, in which ITB discharges show no deterioration of plasma confinement, as shown in Fig. 1.c.

3. Thermal quench plasma energy collapse and timescales.

Coincident with the flattening of the current profile at the disruption, the plasma pressure suffers a major redistribution and a large decrease of the plasma energy occurs. In this study, we include the two phases (energy density redistribution and collapse) in the so-called thermal quench, in contrast to previous studies [3, 4]. Experimental evidence indicates that a substantial energy loss from the plasma and energy fluxes to PFCs can take place in both phases. An example of the re-distribution and collapse of the electron temperature profile at the thermal quench of a JET disruption is shown in Fig. 3.a. The temperature redistribution phase takes place in ~ 1 ms and the final collapse in ~ 1 ms. Fig. 3.b shows the collapse of the central electron temperature for two JET disruptions (one is that of Fig. 3.a) and the associated particle fluxes to the divertor. In some disruptions, such as that of Fig. 3.a, significant fluxes on PFCs are only measured in the final temperature profile collapse phase and not in the redistribution phase [9]. However, in other disruptions, the dominant fluxes are measured at the redistribution phase, as shown in Fig. 3.b for discharge 60636. Due to this complicated energy flux evolution at the thermal quench, the energy flux to the divertor during the thermal quench can be single or multiply peaked in time, as shown in Figs. 3.c and 3.d for ASDEX Upgrade [11]. Furthermore, the characteristic timescales for the thermal quench divertor power fluxes can be different from the electron temperature collapse and redistribution timescales at the thermal quench, in contrast to assumptions in previous studies [3, 4]. This is illustrated in Fig. 4 for experiments in ASDEX Upgrade [11], DIII-D [10, 12], FTU [13], JET [7, 9], MAST [8] and TEXTOR [14]. In this figure, the characteristic timescale for the collapse of the plasma has been determined following the same approach as in [9] and the duration of the thermal quench divertor power flux following the approach in [11]. Both timescales show a large spread, which is in part associated with the disruption type but also to the intrinsic variability of these timescales for virtually identical disruptions [9, 11]. This is associated with the detailed time evolution of the plasma collapse in every disruption, as described before. Despite this variability, the timescales for the plasma energy collapse and the thermal quench divertor energy fluxes are longer for larger devices, confirming the favourable size scaling of these timescales identified in the initial ITER studies [4]. For most tokamaks, the duration of the thermal quench divertor power flux pulse is longer than the main plasma thermal collapse as determined by the ECE, which was the timescale originally used to derive the thermal quench load specifications in ITER [4]. No obvious correlation of either timescale with the pre-disruptive plasma parameters, such as plasma energy, temperature, etc., has been identified within the existing experimental data in JET and ASDEX Upgrade [9, 11]. A histogram of the divertor power flux timescale for a large database of ASDEX Upgrade disruptions is shown in Fig. 5.a [11]. The only clear difference in timescales identified so far refers to the main plasma energy thermal quench collapse for high $\vec{\nabla}_r p$ ITB disruptions in JET [9] and DIII-D [12], which are particularly short (~ 100 μs). Despite this, the characteristic time for energy flux to the divertor during the thermal quench in this case is not significantly different from other disruption types in JET, as shown in Fig. 5.b. It is important to note that, contrary to ELMs, the divertor target surface temperature in ITER is expected to exceed substantially the material damage threshold. In these conditions material erosion is mostly determined by the length of time during which the surface temperature is beyond the damage threshold [15]. Therefore, in the studies of disruptions for ITER, the relevant timescale is the duration of the power flux time and not only of the rise phase, as it is the case for ELM studies [15].

The power flux to the divertor during the thermal quench has a very broad footprint for all disruption types. This usually leads to an almost uniform (within a factor of 2) power flux on the whole divertor target during the thermal quench and, as a consequence, to a much lower temperature increase than would be expected otherwise. This observation is opposite to that reported from limiter tokamaks, in which no significant broadening of the power flux to the limiter is observed at the thermal quench [14, 16]. An example of the power flux

distribution on various tiles of the divertor for JET [7] and ASDEX Upgrade [11], illustrating this point, is shown in Fig. 6.a. An overview of the normalised (to steady state plasma conditions) thermal quench divertor power flux width in various devices is shown in Fig. 6.b. The broadening seen in divertor discharges decreases substantially the peak power load on the divertor at the thermal quench but leads to significant energy fluxes reaching the main chamber wall PFCs (see ASDEX Upgrade data in Fig. 6.a). This was originally deduced from the JET measurements [17] and has been recently measured in ASDEX Upgrade [11, 18]. This fact, together with observed toroidal asymmetries of the thermal quench divertor power flux during disruptions, makes the disruption global energy balance to be very complex and prevents any conclusive estimate for ITER in this respect. Present estimates of the total energy deposited at the divertor during the thermal quench are in the range 15 – 150 % [6 – 12], the lowest values being typical of high $\bar{\nabla}_r p$ ITB disruptions in JET. In absence of more conclusive studies, we will assume that up to 100% of the thermal quench plasma energy can flow to the divertor during the ITER disruptions.

4. Discussion and expected power fluxes in the thermal quench of ITER disruptions.

The new measurements described in the previous sections call for a re-evaluation of the conditions expected for the average disruptions to be encountered when operating ITER in its reference Q_{DT} = 10 scenario based on the ELMy H-mode. In first place, the average plasma energy at the thermal quench in ITER will be ~ 88 MJ (175 MJ, if no disruption amelioration is applied), i.e., ~ 25 % of the full performance plasma energy. This energy will flow to the divertor over a very large area, which will be typically in the range of 5-10 times the divertor wetted area for power flux in steady-state conditions ($A_{s.s}$), i.e. 18–35 m^2 in ITER. The typical timescale for the thermal quench power pulse, from the data in Fig. 4, is in the range 1.5–3 ms. As a consequence of these factors, the expected divertor energy flux in the average ITER disruption will be ~ 3.3 MJm^{-2}, with a timescale of ~ 2.3 ms. Using the standard deviations in the distribution functions, the lowest and highest thermal quench energy fluxes will be ~ 7.5 MJm^{-2} in ~ 1.5 ms and ~ 1.3 MJm^{-2} in ~ 3.0 ms, respectively.

The characteristic surface temperature rise, which determines the material damage caused by the power flux, can be estimated by the so-called "ablation-melting" parameter $\phi \sim \Gamma_{E.q.}/\sqrt{t_{t.q.}}$, where $\Gamma_{E.q.}$ is the energy flux during the thermal quench and $t_{t.q.}$ is its timescale. For the average ITER disruption, the expected "ablation-melting" parameter will, thus, be in the range 46–129 MJ $m^{-2}s^{-1/2}$, which is about a factor of 3-4 higher than that required to cause carbon ablation (35 MJ $m^{-2}s^{-1/2}$) and tungsten melting (40 MJ $m^{-2}s^{-1/2}$) [15]. While this is by no means a low energy flux, it is more than an order of magnitude lower than that expected under the previous assumptions ($W_{plasma\ t.q.}$ = 350 MJ, $A_{t.q.}$ = 3 $A_{s.s.}$, $t_{t.q.}$ = 1 ms). As a consequence, the expected divertor target lifetime under these "revised" most frequent disruptions in ITER is significantly longer than previously estimated, as shown in Fig. 7.

5. References.

[1] Federici, G., et al., J. Nucl. Mat. **313-316** (2003) 11.

[2] Würz, H., et al., J. Nucl. Mat. **307-311** (2002) 60.

[3] Wesley, J., et al., Fusion. Engineering 1997 (Proc 17th Symp. San Diego, 1997), Vol.1, IEEE, Piscataway, USA (1998) 483.

[4] ITER Physics Basis, Nucl. Fusion **39** (1999) 2137.

[5] Kukushkin, A., et al., Nucl. Fusion **42** (2002) 187.

[6] Riccardo, V. et al., Plasma Phys. Control. Fusion **44** (2002) 905.

[7] Paley, J., et al., 16th PSI Conference, Portland, USA, 2004. To be published in J. Nucl. Mat.

[8] Counsell, G., et al., Proc. 31st European Physical Society Conference on Controlled Fusion and Plasma Physics, London, UK, 2004. P4-185.

[9] Riccardo, V., et al., submitted to Nucl. Fusion.

[10] Whyte, D., G., et al., J. Nucl. Mat. **313-316** (2003) 1239.

[11] Pautasso, G., et al., Proc. 31st European Physical Society Conference on Controlled Fusion and Plasma Physics, London, UK, 2004. P4-132.

[12] Whyte, D., G., et al., submitted to Fus. Science & Technology.
[13] Ciotti, M., et al., J. Nucl. Mat. **220-222** (1995) 567.
[14] Finken, K.H. , et al., Nucl. Fusion **40** (2000) 339.
[15] Federici, G. et al., Plasma Phys. Control. Fusion **45** (2003) 1523.
[16] Ciotti, M., et al., J. Nucl. Mat. **266-269** (1999) 1023.
[17] Matthews, G., et al., Nucl. Fusion **43** (2003) 999.
[18] Eich, T., et al., 16th PSI Conference, Portland, USA, 2004. To be published in J. Nucl. Mat.

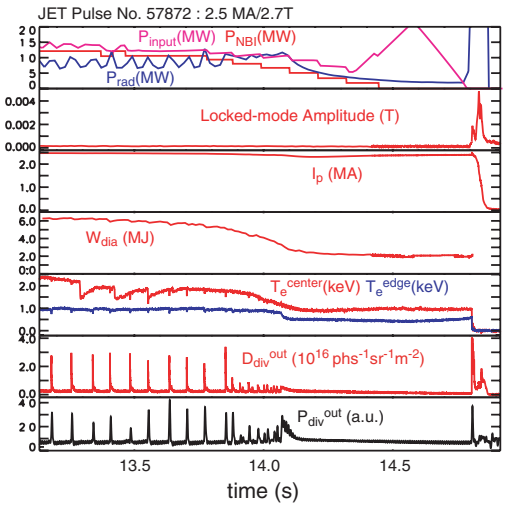

Figure 1.a. Plasma parameters in the approach to a disruption in JET caused by a density limit at the switch-off of the additional heating. From top to bottom : total input power, neutral beam heating power and radiated power, amplitude of the locked-mode, plasma current, plasma energy, electron temperature at the plasma centre and at the edge, outer divertor D_α emission and maximum power flux at the outer divertor.

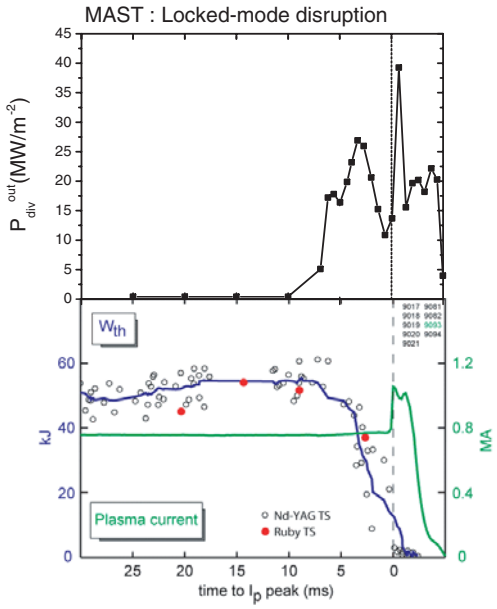

Figure 1.b. Plasma parameters in the approach to a disruption in MAST caused by a locked mode. From top to bottom : maximum power flux at the outer divertor, plasma current and plasma energy.

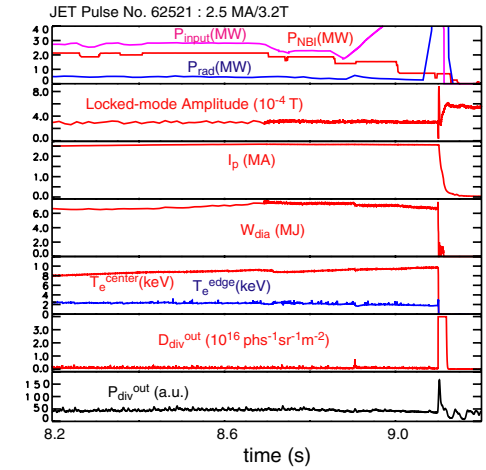

Figure 1.c. Plasma parameters in the approach to a disruption in JET caused by an excessive pressure gradient in an ITB discharge. From top to bottom : total input power, neutral beam heating power and radiated power, amplitude of the locked-mode, plasma current, plasma energy, electron temperature at the plasma centre and at the edge, outer divertor D_α emission and maximum power flux at the outer divertor.

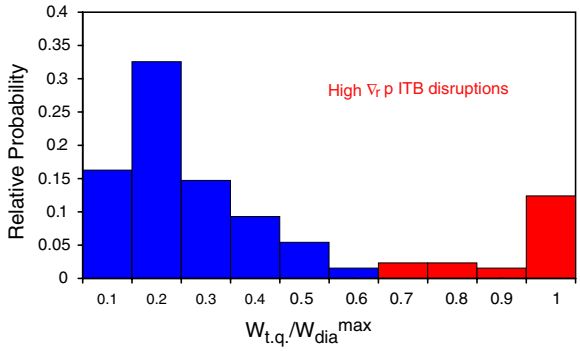

Figure 2.a. Distribution probability of the normalised plasma energy at the thermal quench (versus the energy of the full performance plasma) for a set of JET disruptions. Only for ITB discharges, in which the plasma disrupts due to an excessive peaking of the pressure profiles, the plasma energy at the thermal quench is comparable to that at full performance.

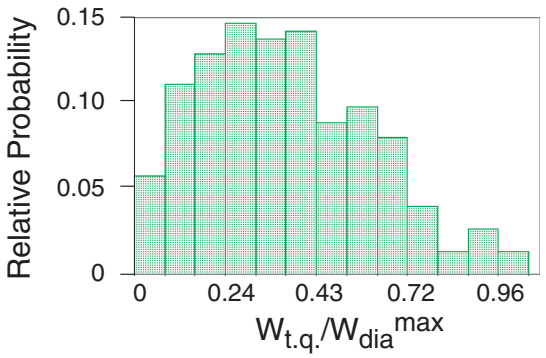

Figure 2.b. Distribution probability of the normalised plasma energy at the thermal quench (versus the energy of the full performance plasma) for a set of ASDEX Upgrade disruptions.

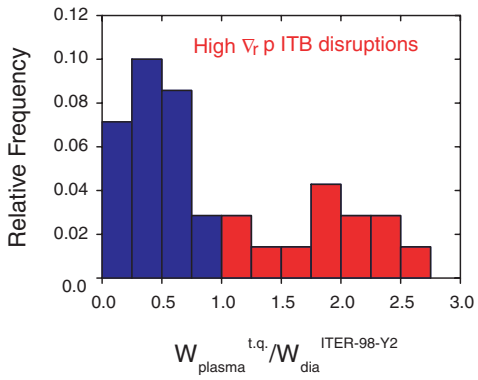

Figure 2.c. Distribution probability of the normalised plasma energy at the thermal quench (versus the energy of the plasma if it were a H-mode at the time of the thermal quench) for a set of JET disruptions.

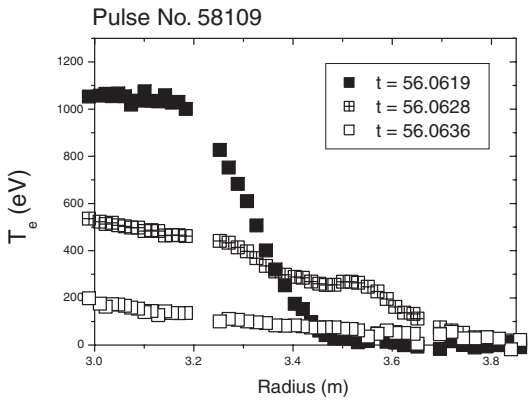

Figure 3.a. Electron temperature profiles at the thermal quench in a JET disruption showing the redistribution and collapse phases.

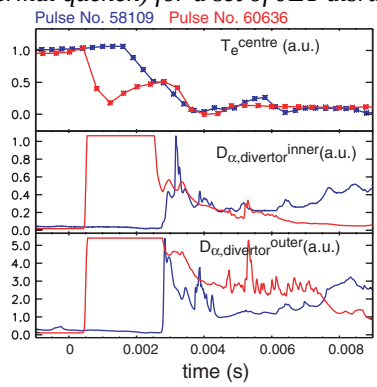

Figure 3.b. Time evolution of the central electron temperature and inner and outer divertor D_α emission during the thermal quench for two JET disruptions.

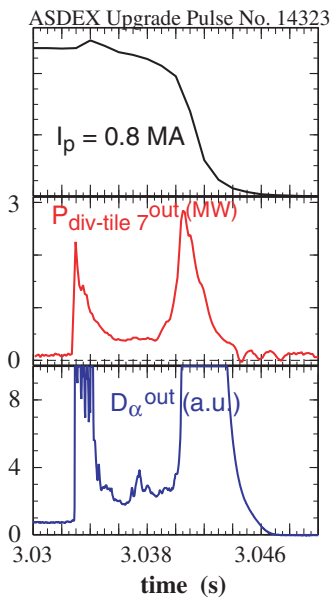

Figure 3.c. Power and particle fluxes to the outer divertor during a disruption in ASDEX Upgrade (the first large peak corresponds to the thermal quench and the second to the current quench). For this disruption, the plasma losses its energy leading to the measured power and particles fluxes in a single step.

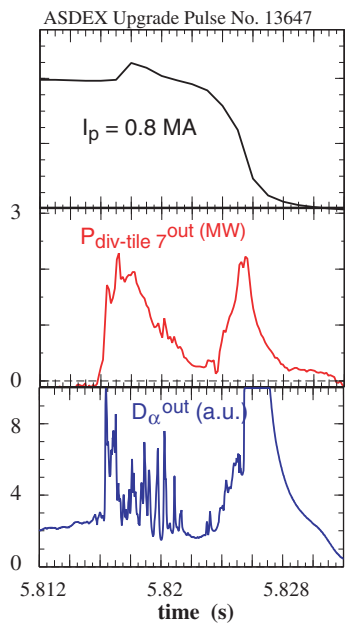

Figure 3.d. Power and particle fluxes to the outer divertor during a disruption in ASDEX Upgrade (the first large peak corresponds to the thermal quench and the second to the current quench). For this disruption the plasma losses its energy leading to the measured power and particles fluxes in various steps.

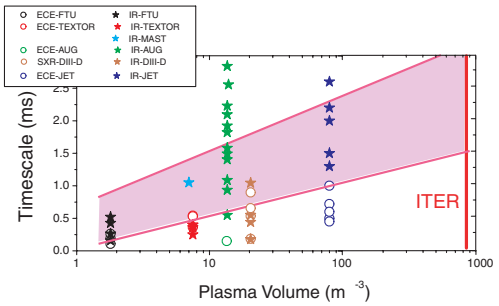

Figure 4. Timescales for the plasma collapse at the thermal quench, as determined by the central ECE temperature measurements and by the duration of the power flux pulse at the divertor for various tokamak experiments and disruption types.

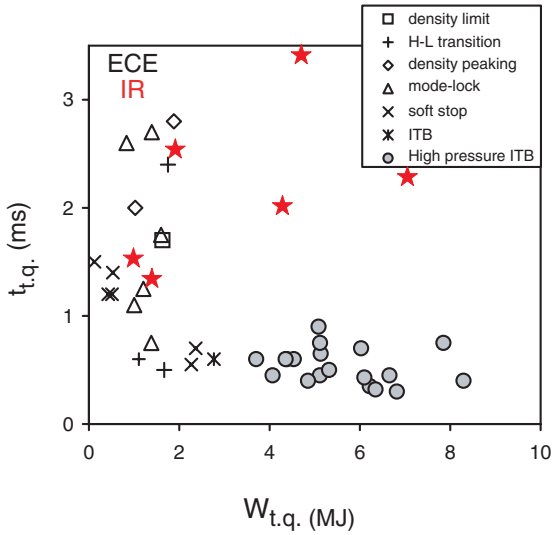

Figure 5.b. Timescales for the plasma collapse at the thermal quench, as determined by the central ECE temperature measurements and by the duration of the power flux pulse at the divertor for various types of disruptions in JET.

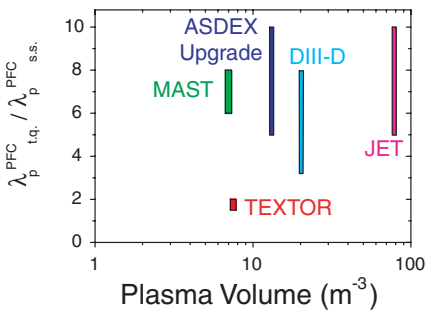

Figure 6.b. Ratio of the divertor power flux width at the thermal quench to that during steady state plasma conditions for various tokamak devices, showing the large broadening of the power flux width in divertor tokamaks, which is absent in limiter tokamaks.

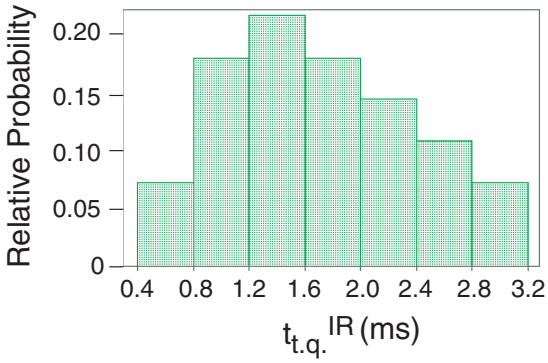

Figure 5.a. Probability distribution function of the divertor power flux duration at the thermal quench of ASDEX Upgrade disruptions.

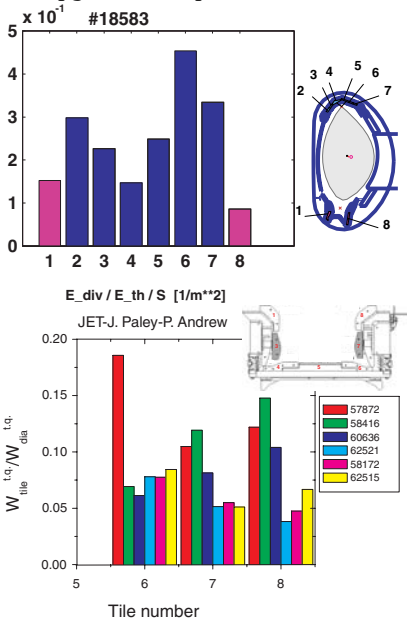

Figure 6.a. Distribution of the plasma energy at the thermal quench on various divertor tiles in ASDEX Upgrade and JET. The energy distribution is very broad with typical e-folding lengths similar to the spatial extent of the divertor itself.

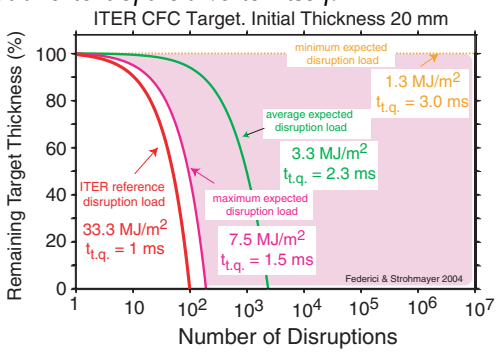

Figure 7. Expected reduction of the ITER carbon divertor target thickness caused by carbon ablation following disruption thermal quench energy fluxes for four energy flux levels/thermal quench durations.